



Iranian Research Organization  
for Science and Technology  
(IROST)

Advances  
Environmental  
Technology



Journal home page: <https://aet.irost.ir>

# Polydopamine functionalized halloysite nanotubes incorporated polyethersulfone hollow fiber membranes for the removal of arsenic (as-v) from water

Mruthyunjaya Swamy D.<sup>a</sup>, Arun M. Isloor<sup>\*a</sup>, Sooraj S. Nayak<sup>a</sup>, Muttanna Venkatesh<sup>a</sup>, Vijayendra Shetti<sup>b</sup>

<sup>a</sup>Membrane and Separation Technology Laboratory, Department of Chemistry, National Institute of Technology Karnataka, Surathkal, India.

<sup>b</sup>Department of Chemistry, National Institute of Technology Karnataka, Surathkal, India.

## ARTICLE INFO

Document Type:  
Research Paper

Article history:  
Received 22 October 2024  
Received in revised form  
03 April 2025  
Accepted 03 April 2025

Keywords:  
Polydopamine functionalized  
halloysite nanotubes  
(FHNTs)  
Hollow fibre membrane  
Phase inversion  
Heavy metal rejection

## ABSTRACT

Polyethersulfone (PES) based hollow fiber membranes containing polydopamine-functionalized halloysite nanotubes (FHNTs) were fabricated in different concentrations employing a dry-wet approach and using phase inversion methodology. Thus, the prepared nanocomposite hollow fiber membranes were characterized using FE-SEM (Field Emission Scanning Electron Microscopy), AFM (Atomic Force Microscopy), ATR-IR, Zeta Potential, and contact angle for studying membrane surface morphology, topography, presence of functional groups, surface charge, and hydrophilicity, respectively. Filtration studies such as pure water permeability, fouling resistance, and heavy metal rejection (arsenic) were performed at a 2 bar pressure. It was found that as the concentration of FHNTs increased in the membrane, the pure water flux also increased, indicating an increase in hydrophilicity. The membrane PPD-4, with the highest percentage of FHNTs, showed the maximum heavy metal removal. It was confirmed by the values of arsenic removal by the membranes containing FHNTs at 0 wt%, 0.2 wt%, 0.6 wt%, and 1 wt% that were found to be 24.80%, 33.18%, 35.54%, and 39.65%, respectively.

## 1. Introduction

In recent decades, rapid population growth has been attributed to industrialization and urbanization. However, due to the limited availability of natural resources, humans have struggled to manage the environment and

ecosystem effectively. As a result, the quality of life for many living beings is declining. Anthropogenic activities have led to the destruction and pollution of natural resources, impacting all life forms in the vicinity. One of the major challenges humans face today is the availability of clean water. Effluents

\*Corresponding author Tel.: +919448523990

E-mail: isloor@yahoo.com

DOI: 10.22104/AET.2025.7186.1978

COPYRIGHTS: ©2024 Advances in Environmental Technology (AET). This article is an open access article distributed under the terms and conditions of the Creative Commons Attribution 4.0 International (CC BY 4.0) (<https://creativecommons.org/licenses/by/4.0/>)

from various industries, such as textiles, pharmaceuticals, automotive, and metallurgy, are contaminating water resources with harmful substances. When organisms consume this polluted water, they become susceptible to life-threatening diseases. One significant contaminant is arsenic [1].

Arsenic, a heavy metal, enters water sources due to both natural (geogenic) and human (anthropogenic) activities. Prolonged exposure to or consumption of arsenic-contaminated water is known to cause severe health issues. The International Agency for Research on Cancer (IARC) classifies arsenic as a class-A carcinogen and a poison to humans. Arsenic in water typically exists in an inorganic form, mainly as two species: Arsenite (+3) and Arsenate (+5). Among these, Arsenite is more toxic and more challenging to remove due to its high solubility in water. Various techniques have been reported globally for the removal of arsenic from water, including oxidation, phytoremediation, flocculation, coagulation, ion exchange processes, and membrane filtration. However, many of these methods have limitations and may produce toxic sludge. In contrast, membrane filtration is considered a safer option compared to other techniques. Numerous studies on membrane filtration have shown promising results for the effective removal of arsenic [2-6].

The advancement of material science has significantly enhanced the potential of membrane technology. The wide variety of materials available for membranes imparts desirable properties, allowing for their use in specific applications. Filler-incorporated membranes have demonstrated numerous applications across different fields; one notable filler is clay nanotubes. These nanotubes are prominent fillers due to their larger surface area, excellent physicochemical properties, cost-effectiveness, and more. Halloysites are particular naturally occurring clay materials with nano tubular structures consisting of an aluminosilicate layer comprising of a profused amount of Si-OH and Al-OH groups; it is the reason for their overall negative charge, high hydrophilicity and ease of modification, which gives them the potential to replace expensive nanofillers such as carbon nanotubes (CNTs) and boron nitrides nanotubes [7]. Reports are stating that halloysite

incorporated membranes have exhibited very good water permeation properties and increased flux capacity [8,9].

Halloysite nanotubes are naturally occurring inorganic compound aluminosilicate clay minerals with the chemical formula  $\text{Al}_2\text{Si}_2\text{O}_5(\text{OH})_4 \cdot n\text{H}_2\text{O}$  [10]. Inorganic additives are used to enhance the anti-fouling properties and hydrophilicity of polymer membranes during the removal of contaminants from water. Adding these inorganic materials to the membranes improves their thermal and mechanical stability, chemical resistance, water uptake, and antifouling characteristics [11]. The halloysite nanotube's outer surface is made of siloxane groups (Si-O-Si), whereas aluminol groups are present at the inner surface and edges of the HNTs. The hollow tubular structure of halloysite is the result of the difference in alignment of two layers, namely a tetrahedral sheet of silicate and an octahedral sheet of alumina. HNTs have a very low agglomeration tendency and can be easily dispersed in polar polymers. Recently, many researchers have reported strong flame retardancy and high thermal stability of polymeric materials in the presence of HNTs [12].

In the present study, the fabricated polydopamine functionalized halloysite nanotubes were incorporated in PES hollow fiber membranes; polyethersulphone was chosen as the base polymer because it is known as the best polymeric material; it is used in various industries because of its high chemical, mechanical, and thermal stability. Also, it can dissolve in a wide spectrum of solvents [13-16]. Membrane technology is a beneficial and trustworthy method for removing contaminants from water due to its low-cost effectiveness, operational ease, flexibility, and selective separation with smaller requirements of footprints compared to other technologies like adsorption, flocculation, coagulation, and advanced oxidation. Various types of membranes have been employed in micro, ultra, and nano-filtration, pervaporation, and reverse osmosis for removing the pollutants. Ultrafiltration membranes are tailored mainly to eliminate arsenic ions from water [17]. Antifouling UF membranes are studied by using Bovine Serum Albumin (BSA) [18]. The UF membrane's surface is modified to reject the pollutants by the size exclusion process; this size exclusion mechanism

eliminates the pollutants from water through the porous UF membrane. The charges on the membranes highly influence the rejection properties and antifouling nature of UF membranes, and the membrane charge may be negative or positive; it varies based on specific modification methods. The PES UF membrane incorporated by the additives helps to increase flux, antifouling tendency, and rejection properties during the purification process [19]. In this study, a PES membrane with 1% FHNTs achieved a 39.65% arsenic removal at a 2 bar pressure due to its antifouling and good rejection properties.

Even though there is a lot of advancement in water purification through membrane technology, mainly in the case of arsenic removal, several challenges persist [20]. Conventional methods like coagulation, ion exchange, and oxidation are limited by their insufficiency and the generation of secondary pollutants like toxic sludge. While membrane filtration is a promising technology, it still faces problems with fouling, insufficient rejection rates in arsenite ( $As^{+3}$ ), and lower flux.  $As^{+3}$  and  $As^{+5}$  are the predominant toxic ionic species in water, but compared to  $As^{+5}$ ,  $As^{+3}$  is very difficult to remove from water [21]. Recently, researchers have reported that the incorporation of halloysite nanotubes into the membrane improves the antifouling nature, rejection rate, and permeability. However, research on polydopamine halloysite nanotubes incorporated in polyethersulphone is highly limited. Also, the role of functionalized HNTs or nanomaterials on membrane structural surface behavior, performance, and arsenic removal has not been completely explored.

Additionally, membrane stability and water permeability have been reported. However, there is a lack of comprehensive studies on how different or varying concentrations of FHNTs impact the membrane antifouling behavior, removal of contaminants, and overall filtration process, especially in the case of arsenic removal. Also, the interaction between the surface charges of modified membranes with FHNTs and their role in the ultrafiltration process performance has remained underexplored. Thus, a gap exists due to insufficient information on how polydopamine functionalized halloysite nanotubes are optimized

within PES membranes to improve arsenic removal, fouling resistance behavior, and overall water filtration and contamination removal performance. So, this study mainly focused on and investigated how varying concentrations of FHNTs affected the PES membrane characteristics and arsenic removal efficiency in water purification. Polydopamine functionalized HNTs incorporated in PES membranes by phase separation methods with different composition and their effect on membrane structure and performance were analyzed in detail. Various characterization techniques and filtration studies were used: SEM, AFM, Zeta potential of the membrane, water uptake study, contact angle measurements, antifouling studies, pure water permeability analysis, and heavy metal rejection studies.

## 2. Material and Methods

### 2.1 Materials

Polyethersulphone (PES) was acquired from the Solvay Company, Belgium. The polyvinylpyrrolidone (PVP), N-methyl-2-pyrrolidone (NMP), halloysite nanotubes, dopamine, tris (hydroxymethyl) aminomethane, and standard arsenic III solution (1000mg/ml) were purchased from Sigma, India. The Bovine Serum Albumin (66,000 g/mol) was purchased from Loba Chemicals Company, India.

### 2.2 Preparation of Polydopamine Functionalized HNTs (FHNTs)

A specific quantity of HNTs was diffused in de-ionized water and sonicated for about 30 minutes to make it into a suspension. The pH of the above-prepared suspension was fixed to pH 8.8 using a tris (hydroxymethyl) aminomethane base (THAM); dopamine was then added and stirred at 30°C for 6 hrs to obtain HNTs coated with black insoluble polydopamine. The above-modified HNTs were collected by centrifugation and washed multiple times with water until the supernatant became colorless, as illustrated in Figure 1 [22].

### 2.3 Fabrication of the hollow fiber membrane

Polydopamine functionalized halloysite nanotubes incorporated PES hollow fiber membranes were fabricated employing a dry-wet approach and using phase inversion methodology. Initially, PES and PVP were vacuum-dried at 100°C for 24 hours

to remove the moisture content. To fabricate a hollow fiber membrane, the dope solution was prepared by dispersing the FHNTs in NMP solvent using sonication for 0.5 hours to avoid particle agglomeration. Subsequently, a specific amount of PES and PVP was added to the suspension, which

was then stirred at 60°C for 24 hours to form a homogeneous polymer solution. The doped solution for the neat membrane was prepared using a similar method, although modified HNTs were not incorporated. The composition of the various dope solutions that were prepared is detailed in Table 1.

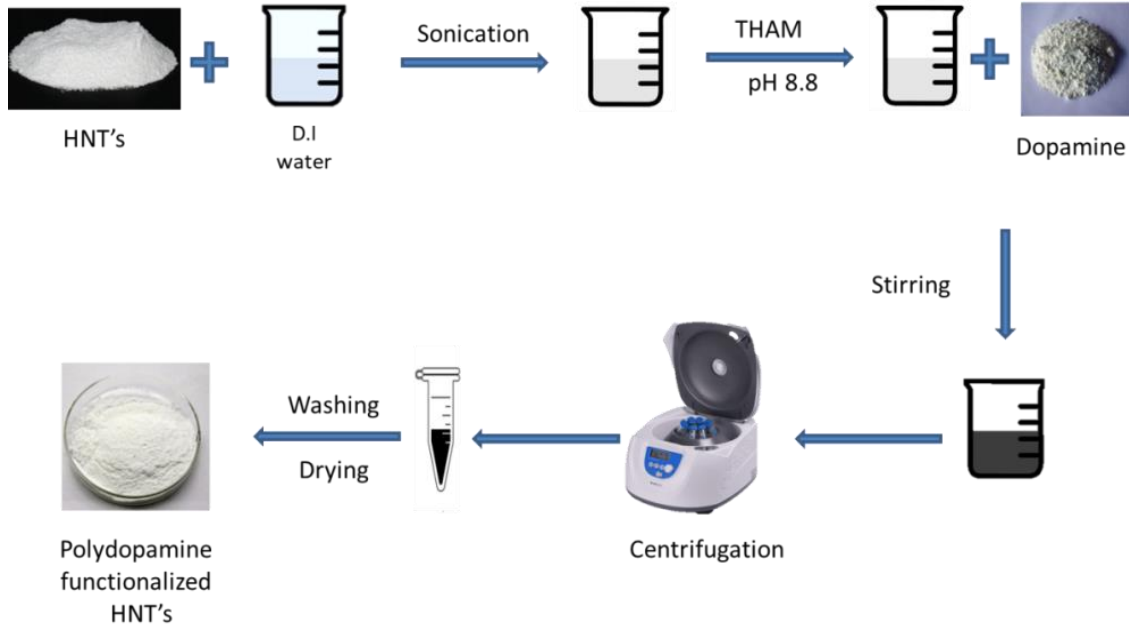


Fig. 1. Schematic diagram of FHNTs synthesis

Table 1. Dope Solution Composition

Membrane	PES (g)	NMP (g)	PVP (g)	FHNTs (g)	$W_{\text{FHNTs}}$ (wt %)
PPD-1	18	80	2	0.0	0
PPD-2	18	80	2	0.0360	0.2
PPD-3	18	80	2	0.0108	0.6
PPD-4	18	80	2	0.1800	1

The above-prepared dope solution was passed to the spinneret through a dope pump; then, deionized water was used as bore liquid and passed through the innermost tubes of the spinneret. The spinneret was placed at a specific distance from the water (non-solvent) bath for fabrication of the membrane through a dry-wet process; specific spinneret parameters were followed during membrane fabrication, shown in Table 2.

The bore liquid and the dope solution emerged through the tip of the spinneret and fell into the water to give hollow fibers. These fibers were passed through two treatment baths of water and finally collected on a winder drum; these membranes were further immersed in a water bath for 24 hours, followed by post-treatment with a

10% glycerol aqueous solution. The membranes were completely dried at room temperature and used for further analysis.

Table 2. Parameters of Spinning Condition

Parameters	Condition
Spinneret OD/ID	1.1/0.5 $\mu\text{m}$
Dope solution	PES/PVP/FHNTs
Bore fluid	De-ionized water
Flow rate of bore fluid	1.5 mL/min
Air gap distance	5 cm
Coagulant	Water
Temperature of coagulant	27°C
Washing bath	Water
Temperature of washing bath	27°C
Take up speed	3 cm/min

## 2.4 Characterization studies

### 2.4.1 ATR-IR spectroscopy study of hollow fiber membranes, FHNTs, and HNTs.

The FHNTs, HNTs, and fabricated membranes were analyzed by ATR-IR Spectroscopy using a Bruker FTIR instrument. The materials and membranes were dried and analyzed for the presence of different functional groups, and the characteristic peaks are discussed in the results and discussion section.

### 2.4.2 Morphological study of the membranes

The cross-sectional morphology was analyzed using a scanning electron microscope (Model: Jeol JSM-6380LA). The cross-section of the membranes was taken by the freeze fracturing technique, where the membranes are dipped in liquid nitrogen for a minute and split immediately to get a uniform section. Later, they were sputtered with a thin layer of gold, and their images were captured using the scanning electron microscope [23].

### 2.4.3 Topographical morphology of the membranes

Atomic force microscopy was used to study the topographical morphology of the hollow fiber membrane. The membranes were cut into a length of 4 cm and adhered to a glass plate; then, they were placed in the sample station of the AFM instrument. Using a tapping mode, the membranes were analyzed for change in the roughness of the surface after the addition of the functional additives.

### 2.4.4 Surface charge properties of the membranes

Surface charge properties of the membrane were studied by using an electrokinetic zeta potential analyzer, which was purchased from Anton Paar. The membranes' surface acquires a charge when they are in an aqueous solution. These surface charges help the membrane to interact with different charged species, thereby helping in the separation process.

### 2.4.5 Hydrophilic/hydrophobic properties of the membranes

The hydrophilic/hydrophobic property of the fabricated membranes was determined by water uptake capacity and measurement of the surface contact angle. Water uptake capacity studies the

swelling nature and bulk hydrophilicity of the membrane, and it is also called the swelling test. In this test, membrane samples were cut into 2cm lengths, weighed, and immersed in distilled water for 24 hours. Later, the samples were wiped with blotting paper, and their wet weight was noted. Then, that membrane sample was dried at 60 °C in a vacuum oven, and its dry weight was noted. The percentage water uptake capacity was calculated using Eq. 1

$$\% \text{ Water Uptake} = \frac{W_w - W_d \times 100}{W_w} \quad (1)$$

Where  $W_w$ -wet is the weight of the membrane sample and  $W_d$ -dry is the weight of the membrane sample. The measurement of the surface contact angle was done using the FTA-200 Dynamic contact angle analyzer. The contact angle of each sample was measured five times to minimize the error, and its average value was reported [24].

### 2.4.6 Pure water permeability study of the fabricated membrane

An incorporated membrane cross-flow filtration system was used to determine the pure water permeability of the FHNTs. For each type of membrane, five hollow fiber membranes were collected and cut into a length of 15 cm and then potted into a steel plug using epoxy resin and dried. These plugs were fixed to a cross-flow filtration cell and kept for compaction for 30 minutes at 2.5 bar pressure. Further, the pressure was reduced to 2 bar, and time-dependent pure water permeability flux was measured every 1 hour for all the compositions of the membrane. Throughout the study, deionized water was used. The pure water permeability was calculated using Eq. 2.

$$J = \frac{Q}{n\pi L \Delta P D_i} \quad (2)$$

where J is pure water flux, n is no. of HF membrane fibers,  $D_i$  is the inner diameter of the HF membrane,  $\Delta P$  is pressure, Q is the volume of water collected, and L is the length of the membrane.

### 3.4.7 Fouling resistivity study of the fabricated membrane

The fouling resistivity character of the membrane was determined by studying the BSA protein permeability for each fabricated membrane using

a cross-flow filtration system. Initially, the membranes were run through compaction for 30 minutes at a 2.5 bar pressure, and the water pressure was reduced to 2 bar pressure. Permeates of pure water flux represented as  $J_{W1}$ , and it was determined using demineralized water for 60 minutes. The BSA permeability study was carried out using a lab-prepared BSA solution of 800 ppm (0.8g/L) at pH  $6.8 \pm 0.2$  for 60 minutes, and the BSA flux permeate was represented as ( $J_P$ ). Further, the membranes were washed carefully, and again, those membranes were studied for pure water permeability for 60 minutes, and the permeate after BSA was represented as  $J_{W2}$ . The antifouling resistance parameters, such as flux recovery ratio (FRR), reversible fouling ( $R_r$ ), and irreversible fouling, were calculated by substituting the values of  $J_{W1}$ ,  $J_{W2}$ , and  $J_P$  in Eqs. 3 to 5.

$$FRR (\%) = \left( \frac{J_{W2}}{J_{W1}} \right) \times 100 \quad (3)$$

$$R_r (\%) = \frac{J_{W2} - J_P}{J_{W1}} \times 100 \quad (4)$$

$$R_{ir} (\%) = \frac{J_{W1} - J_{W2}}{J_{W1}} \times 100 \quad (5)$$

#### 2.4.8 Arsenic rejection study of the fabricated membrane

All the FHNTs incorporated membranes were studied for arsenic rejection analysis from arsenic-containing water. An atomic absorption spectrometer was used to evaluate the arsenic content in the water. The laboratory-made 1 ppm (1mg/L) arsenic solution was prepared at pH  $6.9 \pm 0.2$  and used as feed ( $C_f$ ) for the arsenic rejection analysis. The cross-flow filtration system was used for the analysis, and the pressure was maintained at 2 bar pressure every 60 minutes. Permeate was collected, and its concentration was noted as ( $C_p$ ). The percentage of arsenic rejection was evaluated by substituting the parameters of the feed and the permeate in Eq. 6.

$$\% R = \left( 1 - \frac{C_p}{C_f} \right) \times 100 \quad (6)$$

### 3. Results and discussion

#### 3.1 ATR-IR spectroscopy study of FHNTs and hollow fiber membranes

The ATR-IR spectra of all the membranes with increased concentration of functionalized halloysite nanotubes are illustrated in Figure 2 [21]. The spectra showed S=O strong stretching at  $1149 \text{ cm}^{-1}$  and  $1321 \text{ cm}^{-1}$  and strong C-O stretching at  $1240 \text{ cm}^{-1}$  and  $1076 \text{ cm}^{-1}$ . Aromatic hydrocarbons showed absorptions in the regions  $1600-1585 \text{ cm}^{-1}$  and  $1500-1400 \text{ cm}^{-1}$  due to carbon-carbon stretching vibrations in the aromatic ring. Water was used as a non-solvent during membrane preparation; the membrane was dried, however, some water content was present, so -OH stretching was observable at  $3551 \text{ cm}^{-1}$ . These peaks were due to the polyethersulphone matrix. FHNTs did not show any peaks in the membrane, as they are present in very low concentrations [7]. In Figure 2, the HNTS spectrum shows a peak at  $3688 \text{ cm}^{-1}$  and  $3618 \text{ cm}^{-1}$  due to the vibrational stretching of the -OH group. The peak at  $913 \text{ cm}^{-1}$  was due to the vibrational bending of the Al-OH group, and the  $1022 \text{ cm}^{-1}$  band corresponded to the vibrational stretching of Si-O bonds. After functionalization, the spectrum displayed a broad peak at  $3422 \text{ cm}^{-1}$  corresponding to the -OH group of polydopamine. Also, the peaks at  $3615 \text{ cm}^{-1}$  and  $3688 \text{ cm}^{-1}$  were due to the symmetric and asymmetric stretching vibration of the -NH group. The carbonyl absorption at  $1624 \text{ cm}^{-1}$  confirmed the formation of the polydopamine functionalization of the HNTs.

#### 3.2 Morphology of the membranes

Figure 3 shows cross-sectional images of fabricated neat and functionalized HNTs incorporated hollow fiber membranes. All the membranes showed the typical asymmetric membrane structure comprised of a top skin layer containing finger-like projections and a sponge-like sub-layer consisting of macro voids below it. The skin layer influenced the selectivity, and the sub-layer acted as a supporting layer providing mechanical strength, which increased the membrane permeability and selectivity [23,25].

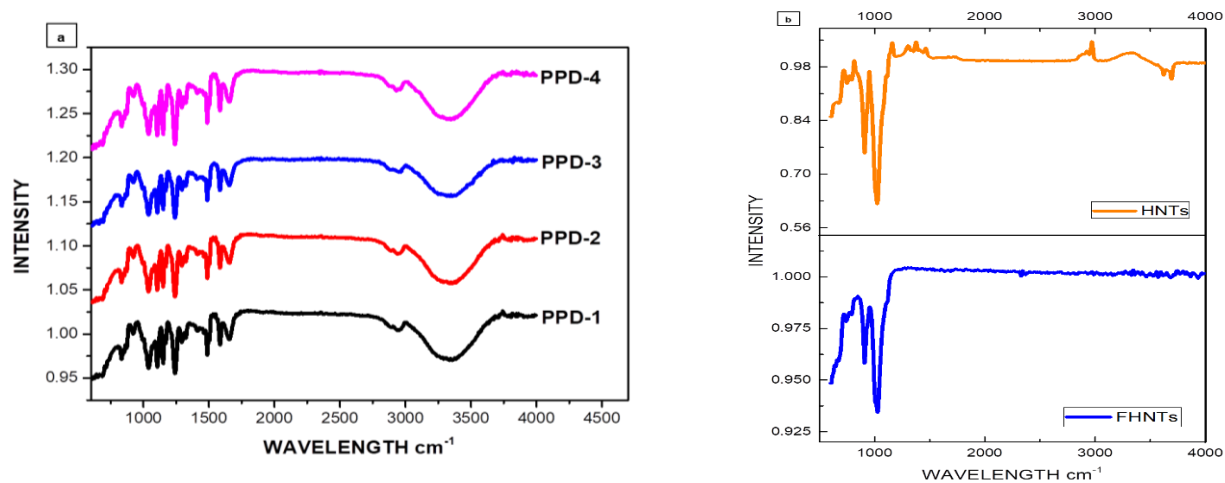


Fig. 2. a) ATR-IR Spectra study of fabricated hollow fiber membranes b) ATR-IR Spectra of HNTs and FHNTs

### 3.3 Topographical morphology of the membranes

Three-dimensional topographical AFM images of the fabricated membranes were captured (Figure 4). The surface roughness parameter ( $R_a$ ) was assessed to determine the roughness of the surface of the membranes. Comparatively, the hollow fiber membranes exhibited morphological changes during the membrane formation. With increasing

nanoparticle composition, the roughness of the membrane decreased. The neat PES membrane exhibited a roughness of 142 nm. As the concentration of FHNTs increased to 0.2%, 0.6%, and 1%, the roughness decreased to 138 nm, 125 nm, and 103 nm, respectively. As a result, the decrease in surface roughness could decrease the fouling rate of the membranes, as the foulants will easily wash off because of the smoothness [26].

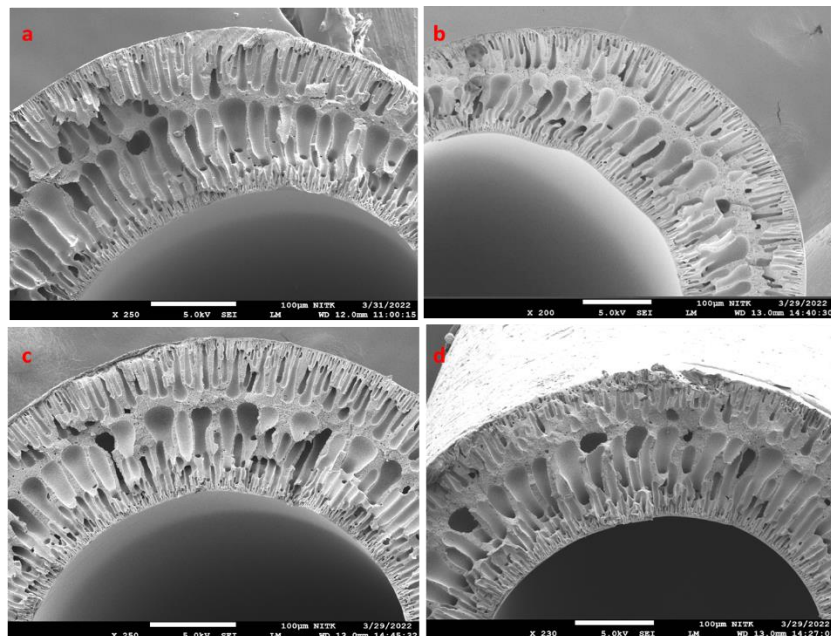


Fig. 3. FE-SEM cross sectional images of HF membranes a) PPD-1 b) PPD-2 c) PPD-3 d) PPD-4

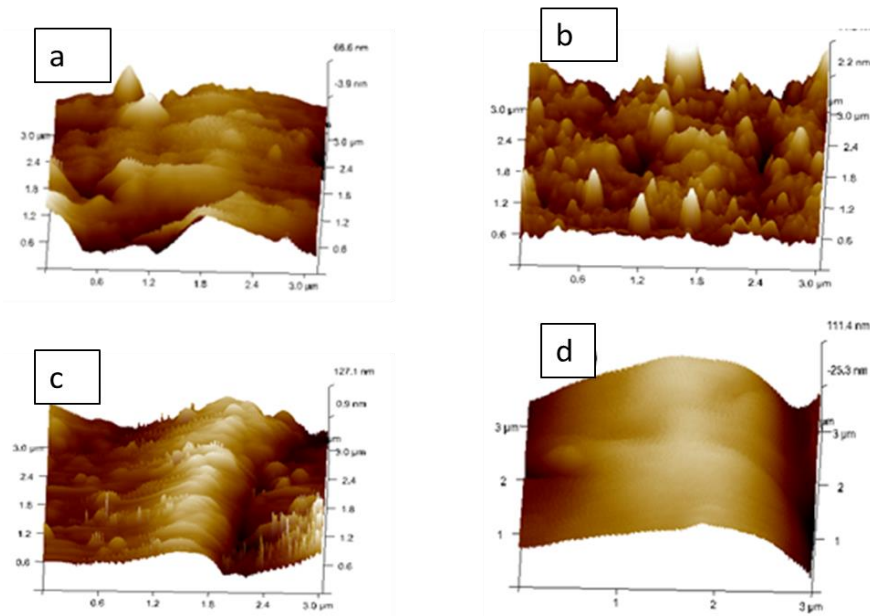


Fig. 4. AFM images of HF membranes - a) PPD-1 b) PPD-2 c) PPD-3 d) PPD-

### 3.4 Surface Charge properties of the membranes

The surface charge of the membrane was assessed through zeta potential for the well-performed membrane PPD-4. Figure 5 shows the graph of zeta potential at different pH levels. The polydopamine functionalized halloysite nanotubes incorporated polyethersulphone hollow fiber membranes showed a negative charge at pH 8.99. The charge was neutralized by adding 0.5 M to get an isoelectric point (IEC) at pH 2.61, inferring that the membrane PPD-4 had a negative surface charge, which would indeed help the membrane to repel negatively charged species [27].

### 3.5 Hydrophilic/hydrophobic properties of the membranes

One of the vital parameters of the membrane for its application in water treatment is the hydrophilic property of the membrane, which can be determined by the water swelling test and contact angle measurement. The hydrophilic sites in the membrane matrix and the membrane morphology determine the percentage of water uptake of the membrane. That is, as the hydrophilic sites increase, the water uptake also increases. The percentage water uptake of all the membranes was determined and presented in Figure 6. Membrane PPD-1 (i.e., neat membrane) showed a water uptake capacity of around 63.41%, and it increased as the functionalized HNTs content

increased; the maximum water uptake of 99% was exhibited by the membrane with the highest FHNTs content of 1% (i.e., PPD-4). The contact angle measurement indicates the water-wetting character and hydrophilic or hydrophobic character of the membranes. Generally, as the angle of contact increases in value, the hydrophobic character of the membrane increases, and as its value decreases, the hydrophilic character of the membrane increases. All the fabricated membranes' contact angle measurement was determined by the sessile drop method. It was observed that as the concentration of FHNTs increased, the hydrophilic character of the membrane also increased (Figure 6). Therefore, it is viable to say that the FHNTs increase the hydrophilic character of the membrane by introducing hydrophilic sites and increasing the surface-wetting character of the membrane matrix [24,28].

### 3.6 Pure water permeability (PWF) study of the fabricated membrane

Cross-flow filtration tests of the membrane indicated that as the concentration of the FHNTs in the membrane increased, the flux capacity of the membrane also increased. This improvement can be attributed to a rise in the number of hydrophilic sites in the membrane matrix, as well as enhanced surface wetting properties. These characteristics facilitate the flow of water through the membrane,



resulting in greater flux. The neat membrane PPD-1 showed low flux when compared to other membranes because of the absence of FHNTs; the overall flux of all the membranes might also be attributed to an increase in the porosity of the

membrane surface due to the leaching out of additives (PVP) during membrane fabrication [21,29,30]. The pure water permeability of the fabricated membranes is presented in Figure 7.

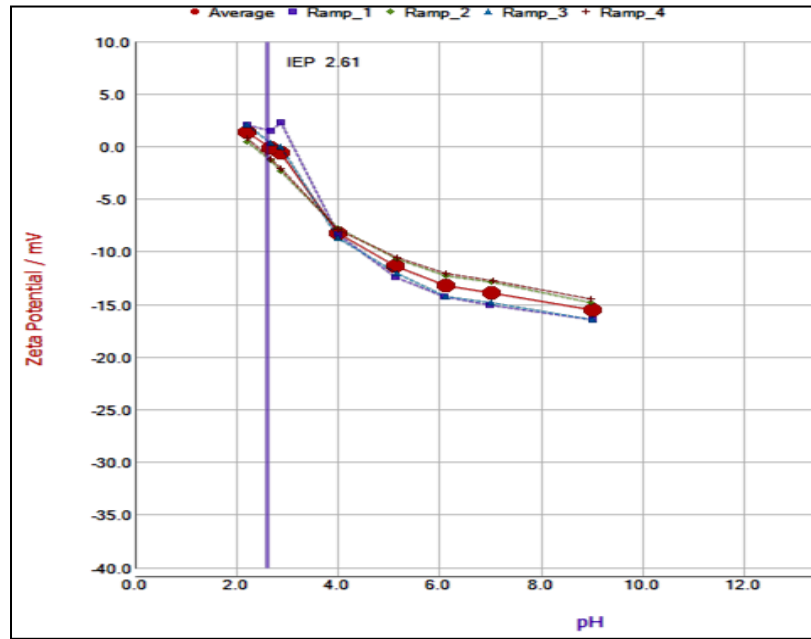


Fig. 5. Zeta potential of PPD-4 membrane at different pH

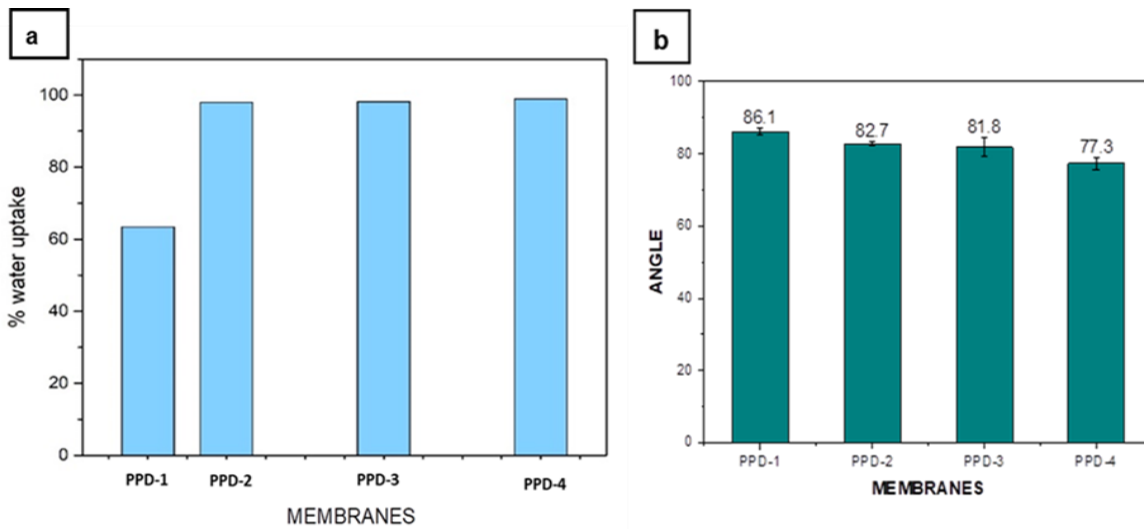


Fig. 6. a) Water Uptake Capacity study b) Contact angle measurement analysis

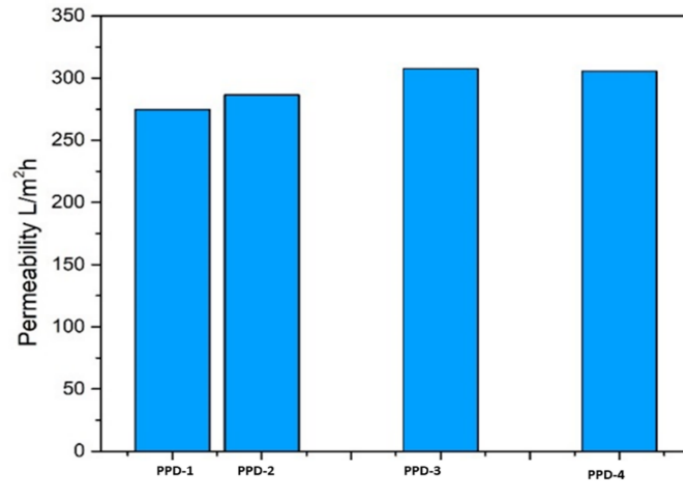


Fig. 7. Pure water permeability study of the membranes

The 1% PDA-HNT/PES membrane exhibited the highest arsenic removal efficiency at 39.65% while maintaining an improved  $150 \text{ L m}^{-2} \text{ h}^{-1}$  compared to the neat  $50 \text{ L m}^{-2} \text{ h}^{-1}$  water flux. This indicated that the 1% PDA-HNT concentration was the most effective option, successfully balancing arsenic removal with filtration efficiency and permeability. When the concentration of PDA-HNT exceeded 1%, it led to the densification of the membrane due to pore blockage. Conversely, if the concentration was less than 1%, it resulted in decreased flux values. Therefore, the optimal concentration of PDA-HNT was 1%, which demonstrated a 200% increase in flux compared to the pristine membrane.

### 3.7 Fouling resistivity study of the fabricated membrane

Membranes are highly susceptible to fouling during their application, which reduces their lifespan. Generally, fouling can be caused by the adsorption of substances (foulants) over the surface of the membrane due to the different types of interaction between the membrane surface and foulants, such as electrostatic interaction, hydrogen bonding effect, and van der Waals forces [31]. Fouling of membranes can be categorized as reversible fouling and irreversible fouling. In reversible fouling, foulants are loosely attached to the membrane surface and can be removed by washing, whereas in irreversible fouling, the foulants are tightly attached to the membrane surface and can only be removed by chemical treatment [32,33].

In the present study, BSA protein was used as a foulant to study the antifouling property of the fabricated membrane. Figure 8 shows the flux of different membranes in three different conditions, including pure water flux ( $J_{W1}$ ), BSA filtration flux ( $J_P$ ), and flux after BSA filtration ( $J_{W2}$ ). It was observed that during BSA filtration, the flux declined due to the adsorption of BSA over the surface of the membrane. The flux recovery ratio (FRR), reversible flux ratio  $R_r$ , and irreversible flux ratio  $R_{ir}$  are shown in Figure 8. Most of the membrane showed very good FRR as most of the foulants were loosely attached to the membrane surface and were removed by simple washing; membranes containing FHNTs showed better FRR as the modified membrane had abundant hydroxyl functional groups, which increased the hydrophilicity, thereby minimizing the hydrophobic-hydrophobic interaction between the foulant and membrane surface. Electrostatic repulsion between the negatively charged BSA protein and the membrane surface could also be the reason for having very good fouling resistance properties.

### 3.8 Arsenic rejection study of the fabricated membrane

Generally, in groundwater, arsenic is in the positively charged form (reductive condition). Therefore, a lab-made arsenate solution was prepared and used for filtration studies to determine the arsenic rejection by fabricated membranes<sup>1</sup>. The rejection percentage of arsenic increased with an increase in FHNT concentration

in the membrane. Figure 9 depicts the rejection studies of all the membranes. Neat membrane PPD-1 showed the least arsenic rejection of 24.8% because the neat membrane was less negatively charged and had less hydrophilic character; the PPD-4 membrane showed the highest rejection percentage of 39.65%. FHNTs were effective in rejecting arsenate ions due to their negatively charged surface, which facilitated electrostatic interactions. Additionally, the -OH groups in the polydopamine enhanced arsenate rejection by acting as chelating agents, enabling strong hydrogen bonding and other secondary interactions with the negatively charged arsenate ions [34,35].

### 3.8.1 Adsorption mechanism

The adsorption mechanism of As (V) onto polydopamine-functionalized halloysite nanotubes (PDA-HNTs) is governed by a combination of electrostatic interactions, hydrogen bonding, and chelation, with the exact contribution of each factor influenced by the material's surface properties and the pH of the solution. Electrostatic interactions play a crucial role, as arsenate (As(V)) exists as an anionic species in water, depending on the pH. At lower pH levels, the protonation of amino groups in PDA imparts a positive charge, enhancing its attraction to negatively charged arsenic species. However, at higher pH levels, deprotonation of these groups can lead to electrostatic repulsion, reducing adsorption efficiency [36]. Additionally, the catechol and amine groups in PDA facilitate hydrogen bonding with arsenic species, particularly under acidic conditions, thereby increasing the adsorption capacity of PDA-HNTs. Chelation also contributes to the adsorption process, as PDA's hydroxyl groups enable the formation of coordination bonds with metal ions, aiding in arsenic capture, especially under neutral to slightly acidic conditions. The surface charge of the membrane, measured through zeta potential analysis, further confirmed the electrostatic nature of arsenic adsorption, with a more positive zeta potential indicating stronger attraction to anionic arsenic species. pH-dependent adsorption studies revealed that arsenic removal was the most effective in the pH range of 4-6, where both electrostatic interactions and hydrogen bonding were optimized [37].

### 3.8.2 Comparative performance of the PDA-HNT/PES membrane with other arsenic removal technologies

The PDA-HNT/PES hollow fiber membrane demonstrates superior arsenic (As-V) removal efficiency compared to traditional technologies. Unlike conventional methods that generate secondary waste or require high energy input, this membrane offers an eco-friendly and efficient alternative for arsenic removal through ultrafiltration, Table 3 indicates the comparative performance of membranes.

### 3.8.3 Thermodynamic and kinetic studies

Table 4 indicates the thermodynamic and kinetic studies of the fabricated membranes.

### 3.8.4 pH-dependent arsenic removal efficiency

Arsenic exists in different forms depending on the pH:  $\text{H}_3\text{AsO}_4$ ,  $\text{H}_2\text{AsO}_4^-$  (arsenate, As(V)) is dominant in neutral to alkaline conditions (pH = 4-10).  $\text{H}_3\text{AsO}_3$  (arsenite, As(III)) is dominant in acidic to neutral conditions (pH = 2-9) the same has been presented in Table 5. Since PDA-HNT/PES membranes remove arsenic through adsorption and filtration, their efficiency is influenced by the pH-dependent charge of polydopamine (PDA) and halloysite nanotubes (HNTs), as well as the speciation of arsenic. The optimal pH range is based on the membrane's zeta potential behavior and arsenic speciation. The optimal pH range for arsenic removal was 6-8, where arsenate (As(V)) was negatively charged, and the membrane surface had moderate electrostatic attraction.

### 3.9 Environmental and economic considerations

Assessing the environmental and economic aspects of utilizing PDA-HNT/PES membranes in water treatment is essential to determining their long-term feasibility. sustainable option due to their natural abundance, non-toxic nature, and biodegradability. Additionally, PDA, inspired by the adhesive proteins found in mussels, is biodegradable, making it a more environmentally friendly alternative to synthetic coatings. From an ecological standpoint, HNTs present a The membranes were manufactured using a dry-wet phase inversion technique, which was energy-efficient and eliminated the need for high-

temperature processing, thereby reducing their overall environmental impact. Moreover, these membranes functioned at a relatively low pressure

(2 bar), which significantly cuts down energy consumption compared to traditional high-pressure filtration methods.

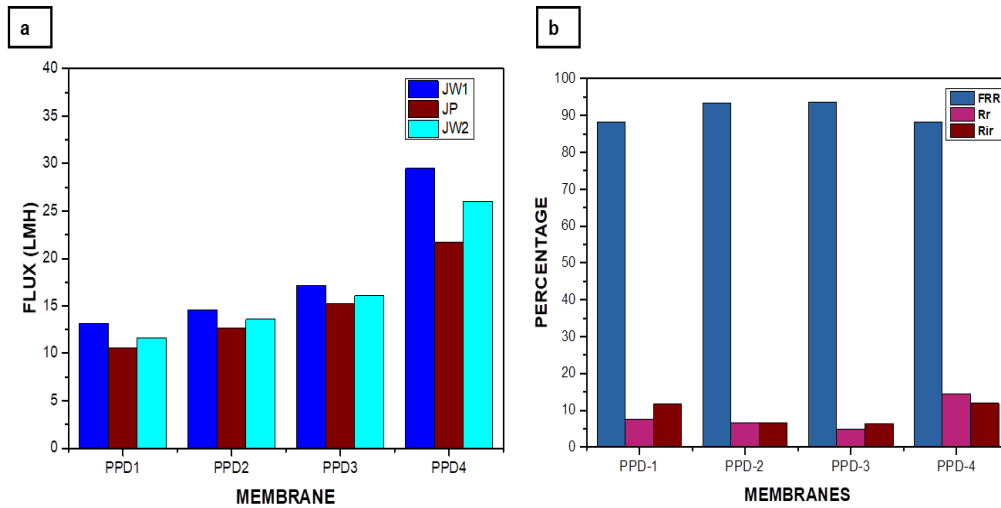


Fig. 8. a) Protein permeability study of the membrane. b) Antifouling Characteristics of the membrane

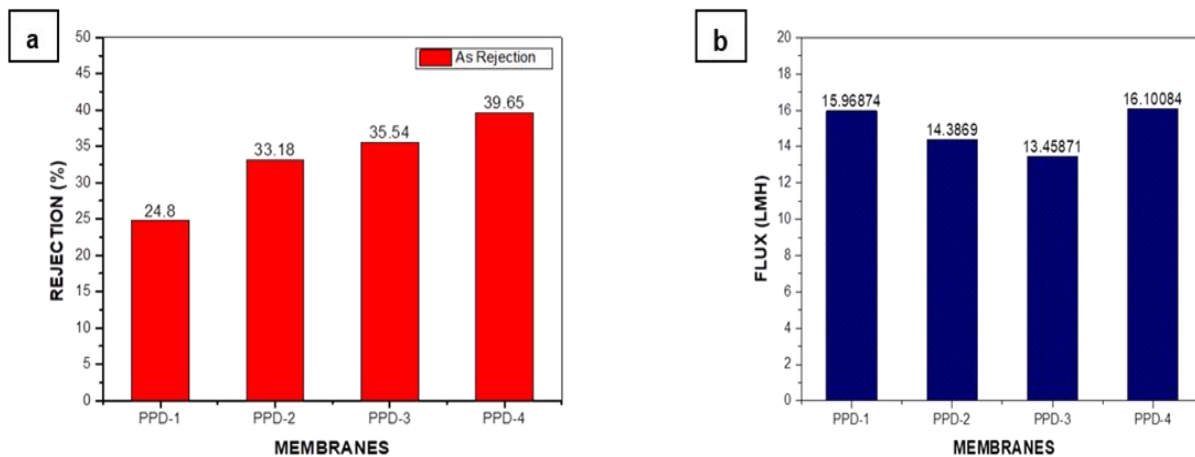


Fig. 9. a) Arsenic Rejection by the membranes, b) Arsenic Rejection Permeability by the membranes

Table 3. Comparison with the other technologies

Technology	Removal efficiency (%)	pH	Cost	Reference
Commercial NF membrane	86-90	3-10	high	[38]
Activate Alumina	95-99	5.5-6.5	Moderate	[39]
Ion-Exchange Resins	>90	6-8	High	[39]

Table 4. Adsorption behavior of As-V onto the membrane

Model	Parameter	Value	Interpretation	Model
Pseudo-first-order	$k_1$ ( $\text{min}^{-1}$ )	0.025	Poor fit (physisorption dominant)	Pseudo-first-order
Pseudo-second-order	$k_2$ ( $\text{g/mg}\cdot\text{min}$ )	0.005	Best fit (chemisorption dominant)	Pseudo-second-order
Langmuir Isotherm	q max ( $\text{mg/g}$ )	15	Monolayer adsorption capacity	Langmuir Isotherm

**Table 5.** pH-Dependent Performance

pH Range	Arsenic Speciation	Membrane Surface Charge	Removal Efficiency
Acidic (2–4)	As(III) (uncharged)	Weakly positive	Low (20%) – Poor electrostatic attraction
Neutral (6–8)	As(V) (charged)	Slightly negative	High (39%) – Favorable electrostatic interaction
Alkaline (9–11)	As(V) (highly charged)	Strongly negative	Moderate (30%) – Electrostatic repulsion affects adsorption

To further reduce their environmental footprint, research into their recyclability and reusability could be beneficial, particularly since the PDA layer may extend the lifespan of the membranes and decrease replacement frequency.

From an economic perspective, PDA-HNT membranes demonstrate strong potential for large-scale manufacturing. Halloysite is a cost-effective material, especially when compared to more expensive nanomaterials like carbon nanotubes or graphene, making it an attractive choice for membrane production. The dry-wet phase inversion process is well-suited for large-scale fabrication, ensuring that the membranes can be produced efficiently for industrial applications. Additionally, PDA-HNT/PES membranes offer superior permeability, enhanced arsenic removal, and improved resistance to fouling, which contribute to lowering operational expenses in water treatment facilities. Their ability to function at lower pressures (2 bar) further reduces energy costs in comparison to high-pressure nanofiltration systems. While the widespread adoption of these membranes will rely on refining the PDA coating process and optimizing fabrication efficiency, their commercial potential remains significant. Conducting pilot-scale evaluations and economic feasibility studies on membrane durability versus operational savings will be critical in determining their long-term viability for cost-effective, large-scale water treatment solutions.

### 3.10 Future work and practical applications

Future research on PDA-HNT/PES membranes for arsenic removal could explore several promising directions to enhance their performance and applicability in real-world water treatment scenarios. One potential area for future investigation is using alternative bio-inspired

functionalization methods. While polydopamine functionalization has shown significant promise, other bio-inspired materials, such as melanin, chitosan, or protein-based coatings, could offer unique properties for improving membrane performance, such as enhanced fouling resistance, selective adsorption, or increased stability under harsh conditions.

Another important avenue of research is testing the membrane's performance under different water sources. Real-world water typically contains a variety of contaminants, including organic matter, salts, and other heavy metals, which can affect membrane efficiency. Investigating how the PDA-HNT/PES membranes perform with varying water compositions, such as municipal wastewater, groundwater, or industrial effluents, will provide valuable insights into their versatility and robustness for broader applications. Studies on the impact of co-contaminants (e.g., lead, mercury) and their effect on arsenic removal efficiency could also provide a more comprehensive understanding of the membrane's overall performance. Additionally, exploring hybrid membrane configurations could further enhance arsenic removal. Combining the PDA-HNT/PES membrane with other filtration technologies, such as activated carbon, electrochemical processes, or adsorptive media, may result in synergies that improve both removal efficiency and fouling resistance. Hybrid systems could also offer advantages in tackling a broader range of contaminants simultaneously, making them more effective for multi-functional water purification systems. Furthermore, future studies could focus on the scalability and commercial viability of these membranes for large-scale applications. Investigating membrane regeneration techniques, operational lifespan, and cost-effectiveness through long-term pilot testing will be crucial for

assessing the membrane's practicality in real-world water treatment plants. It could include assessing the energy consumption and maintenance costs compared to other existing technologies.

#### 4. Conclusions

Polydopamine functionalized halloysite nanotubes incorporated polyethersulphone hollow fiber membranes were successfully fabricated using phase inversion methodology. The well-formed membrane showed an asymmetric composition with a highly dense skin layer containing finger-like projections and below a sub-layer consisting of microvoids. The addition of functionalized HNTs resulted in a membrane with an interconnected finger-like porous structure along with high hydrophilic character, established by contact angle measurement and the swelling test. A pure water permeability study, antifouling study, and heavy metal rejection study indicated an improvement in water flux, flux recovery ratio, and heavy metal rejection with increasing concentration of FHNTs in the membrane. The best result was obtained for the membrane with 1% FHNT concentration (PPD-4), with the maximum arsenic rejection of 39.65 % at 2 bar pressure.

#### Acknowledgements

The authors are grateful to the National Institute of Technology Karnataka (NITK), Surathkal, India, for the lab and instrument facility.

#### References

- [1] Fernández-Luqueño, F., López-Valdez, F., Gamero-Melo, P., Luna-Suárez, S., Aguilera-González, E. N., Martínez, A. I., García-Guillermo, M. D. S., Hernández-Martínez, G., Herrera-Mendoza, R., Álvarez-Garza, M. A., & Pérez-Velázquez, I. R. (2013). Heavy metal pollution in drinking water – a global risk for human health: A review. *African Journal of Environmental Science and Technology*, 7(7), 567–584.
- [2] Mishra, S., Bharagava, R. N., More, N., Yadav, A., Zainith, S., Mani, S., & Chowdhary, P. (2019). Heavy metal contamination: An alarming threat to environment and human health. In R. C. Sobti, N. K. Arora, & R. Kothari (Eds.), *Environmental biotechnology: For sustainable future* (pp. 103–125). Springer Singapore.  
[https://doi.org/10.1007/978-981-10-7284-0\\_5](https://doi.org/10.1007/978-981-10-7284-0_5)
- [3] Mohod, C. V., & Dhote, J. (2013). Review of heavy metals in drinking water and their effect on human health. *International Journal of Innovative Research in Science, Engineering and Technology*, 2(7), 2992–2996.
- [4] Sankhla, M. S., Kumari, M., Nandan, M., Kumar, R., & Agrawal, P. (2016). Heavy metals contamination in water and their hazardous effect on human health: A review. *International Journal of Current Microbiology and Applied Sciences*, 5(10), 759–766.  
<http://dx.doi.org/10.20546/ijcmas.2016.510.082>
- [5] Sonone, S. S., Jadhav, S., Sankhla, M. S., & Kumar, R. (2020). Water contamination by heavy metals and their toxic effect on aquaculture and human health through the food chain. *Letters in Applied NanoBioScience*, 10(2), 2148–2166.
- [6] Zahra, N., & Kalim, I. (2017). Perilous effects of heavy metals contamination on human health. *Pakistan Journal of Analytical & Environmental Chemistry*, 18(1), 1–17.  
<https://doi.org/10.21743/pjaec/2017.06.01>
- [7] Abdullayev, E., & Lvov, Y. (2010). Clay nanotubes for corrosion inhibitor encapsulation: Release control with end stoppers. *Journal of Materials Chemistry*, 20(32), 6681–6687.  
<https://doi.org/10.1039/C0JM00810A>
- [8] Zhang, J., Zhang, Y., Chen, Y., Du, L., Zhang, B., Zhang, H., Liu, J., & Wang, K. (2012). Preparation and characterization of novel polyethersulfone hybrid ultrafiltration membranes bending with modified halloysite nanotubes loaded with silver nanoparticles. *Industrial & Engineering Chemistry Research*, 51(7), 3081–3090.  
<https://doi.org/10.1021/ie202473u>
- [9] Wang, Z., Wang, H., Liu, J., & Zhang, Y. (2014). Preparation and antifouling property of polyethersulfone ultrafiltration hybrid membrane containing halloysite nanotubes grafted with MPC via RATRP method. *Desalination*, 344, 313–320.

- <https://doi.org/10.1016/j.desal.2014.03.040>
- [10] Pandey, G., Tharmavaram, M., & Rawtani, D. (2020). Chapter 15 - Functionalized halloysite nanotubes: An "ecofriendly" nanomaterial in the environmental industry. In C. Mustansar Hussain (Ed.), *Handbook of functionalized nanomaterials for industrial applications* (pp. 417-433). Micro and Nano Technologies, Elsevier.  
<https://doi.org/10.1016/B978-0-12-816787-8.00015-6>
- [11] Satishkumar, P., Isloor, A. M., Rao, L. N., & Farnood, R. (2024). Fabrication of 2D vanadium MXene polyphenylsulfone ultrafiltration membrane for enhancing the water flux and for effective separation of humic acid and dyes from wastewater. *ACS Omega*, 9(24), 25766-25778.  
<https://doi.org/10.1021/acsomega.3c10078>
- [12] Lecouvet, B., Sclavons, M., Bourbigot, S., & Bailly, C. (2013). Thermal and flammability properties of polyethersulfone/halloysite nanocomposites prepared by melt compounding. *Polymer Degradation and Stability*, 98(10), 1993-2004.  
<https://doi.org/10.1016/j.polymdegradstab.2013.07.013>
- [13] Barclay, T. G., Hegab, H. M., Michelmore, A., Weeks, M., & Ginic-Markovic, M. (2018). Multidentate polyzwitterion attachment to polydopamine modified ultrafiltration membranes for dairy processing: Characterization, performance, and durability. *Journal of Industrial and Engineering Chemistry*, 61, 356-367.  
<https://doi.org/10.1016/j.jiec.2017.12.035>
- [14] Nasrollahi, N., Vatanpour, V., Aber, S., & Mahmoodi, N. M. (2018). Preparation and characterization of a novel polyethersulfone (PES) ultrafiltration membrane modified with a CuO/ZnO nanocomposite to improve permeability and antifouling properties. *Separation and Purification Technology*, 192, 369-382.  
<https://doi.org/10.1016/j.seppur.2017.10.034>
- [15] Rezania, H., Vatanpour, V., Arabpour, A., Shockravi, A., & Ehsani, M. (2020). Structural manipulation of PES constituents to prepare advanced alternative polymer for ultrafiltration membrane. *Journal of Applied Polymer Science*, 137(20), 48690.  
<https://doi.org/10.1002/app.48690>
- [16] Zhu, X., Dudchenko, A., Gu, X., & Jassby, D. (2017). Surfactant-stabilized oil separation from water using ultrafiltration and nanofiltration. *Journal of Membrane Science*, 529, 159-169.  
<https://doi.org/10.1016/j.memsci.2017.02.004>
- [17] Kumar, M., Rao, T. S., Isloor, A. M., Ibrahim, G. S., Ismail, N., Ismail, A. F., & Asiri, A. M. (2019). Use of cellulose acetate/polyphenylsulfone derivatives to fabricate ultrafiltration hollow fiber membranes for the removal of arsenic from drinking water. *International Journal of Biological Macromolecules*, 129, 715-727.  
<https://doi.org/10.1016/j.ijbiomac.2019.02.017>
- [18] Kumar, M., Isloor, A. M., Rao, T. S., Ismail, A. F., Farnood, R., & Nambissan, P. M. G. (2020). Removal of toxic arsenic from aqueous media using polyphenylsulfone/cellulose acetate hollow fiber membranes containing zirconium oxide. *Chemical Engineering Journal*, 393, 124367.  
<https://doi.org/10.1016/j.cej.2020.124367>
- [19] Koli, M., & Singh, S. (2023). Surface-modified ultrafiltration and nanofiltration membranes for the selective removal of heavy metals and inorganic groundwater contaminants: A review. *Environmental Science: Water Research & Technology*, 9(11), 2803-2829.  
<https://doi.org/10.1039/D3EW00266G>
- [20] Kumar, M., Isloor, A. M., Todeti, S. R., Nagaraja, H. S., Ismail, A. F., & Susanti, R. (2021). Effect of binary zinc-magnesium oxides on polyphenylsulfone/cellulose acetate derivatives hollow fiber membranes for the decontamination of arsenic from drinking water. *Chemical Engineering Journal*, 405, 126809.  
<https://doi.org/10.1016/j.cej.2020.126809>
- [21] Kumar, M., Isloor, A. M., Todeti, S. R., Ismail, A. F., & Farnood, R. (2021). Hydrophilic nano-aluminum oxide containing polyphenylsulfone hollow fiber membranes for the extraction of arsenic (As-V) from drinking water. *Journal of Water Process Engineering*, 44, 102357.  
<https://doi.org/10.1016/j.jwpe.2021.102357>

- [22] Hebbbar, R. S., Isloor, A. M., Ananda, K., & Ismail, A. F. (2016). Fabrication of polydopamine functionalized halloysite nanotube/polyetherimide membranes for heavy metal removal. *Journal of Materials Chemistry A*, 4(3), 764–774.  
<https://doi.org/10.1039/C5TA09281G>
- [23] Nayak, M., Chandrashekar, A. M., Isloor, A. M., Moslehiani, N., Ismail, N., & Ismail, A. F. (2018). Fabrication of novel PPSU/ZSM-5 ultrafiltration hollow fiber membranes for separation of proteins and hazardous reactive dyes. *Journal of the Taiwan Institute of Chemical Engineers*, 82, 342–350.
- [24] Kingsbury, R. S., Bruning, K., Zhu, S., Flotron, S., Miller, C. T., & Coronell, O. (2019). Influence of water uptake, charge, manning parameter, and contact angle on water and salt transport in commercial ion exchange membranes. *Industrial & Engineering Chemistry Research*, 58(40), 18663–18674.  
<https://doi.org/10.1021/acs.iecr.9b03200>
- [25] Anadão, P., Sato, L. F., Montes, R. R., & De Santis, H. S. (2014). Polysulphone/montmorillonite nanocomposite membranes: Effect of clay addition and polysulphone molecular weight on the membrane properties. *Journal of Membrane Science*, 455, 187–199.  
<https://doi.org/10.1016/j.memsci.2013.12.081>
- [26] Bagheripour, E., Moghadassi, A. R., Parvizian, F., Hosseini, S. M., & Van der Bruggen, B. (2019). Tailoring the separation performance and fouling reduction of PES based nanofiltration membrane by using a PVA/Fe<sub>3</sub>O<sub>4</sub> coating layer. *Chemical Engineering Research and Design*, 144, 418–428.  
<https://doi.org/10.1016/j.cherd.2019.02.028>
- [27] Ibrahim, G. P. S., Isloor, A. M., Inamuddin, Asiri, A. M., Ismail, A. F., Kumar, R., & Ahamed, M. I. (2018). Performance intensification of the polysulfone ultrafiltration membrane by blending with a copolymer encompassing a novel derivative of poly(Styrene-Co-Maleic Anhydride) for heavy metal removal from wastewater. *Chemical Engineering Journal*, 353, 425–435.  
<https://doi.org/10.1016/j.cej.2018.07.098>
- [28] Kadhom, M., & Deng, B. (2019). Thin film nanocomposite membranes filled with bentonite nanoparticles for brackish water desalination: A novel water uptake concept. *Microporous and Mesoporous Materials*, 279, 82–91.  
<https://doi.org/10.1016/j.micromeso.2018.12.020>
- [29] Chou, S., Wang, R., Shi, L., She, Q., Tang, C., & Fane, A. G. (2012). Thin-film composite hollow fiber membranes for pressure retarded osmosis (PRO) process with high power density. *Journal of Membrane Science*, 389, 25–33.  
<https://doi.org/10.1016/j.memsci.2011.10.002>
- [30] Veríssimo, S., Peinemann, K. V., & Bordado, J. (2005). New composite hollow fiber membrane for nanofiltration. *Desalination*, 184(1-3), 1-11.  
<https://doi.org/10.1016/j.desal.2005.03.069>
- [31] Rana, D., & Matsuura, T. (2010). Surface modifications for antifouling membranes. *Chemical Reviews*, 110(4), 2448–2471.  
<https://doi.org/10.1021/cr800208y>
- [32] Lu, X., Peng, Y., Qiu, H., Liu, X., & Ge, L. (2017). Anti-fouling membranes by manipulating surface wettability and their anti-fouling mechanism. *Desalination*, 413, 127–135.  
<https://doi.org/10.1016/j.desal.2017.02.022>
- [33] Jhaveri, J. H., & Murthy, Z. V. P. (2016). A comprehensive review on anti-fouling nanocomposite membranes for pressure driven membrane separation processes. *Desalination*, 379, 137–154.  
<https://doi.org/10.1016/j.desal.2015.11.009>
- [34] Zakhari, R., Derco, J., & Čácho, F. (2018). An overview of main arsenic removal technologies. *Acta Chimica Slovaca*, 11(2), 107–113.  
<https://doi.org/10.2478/acs-2018-0016>
- [35] Shih, M. C. (2005). An overview of arsenic removal by pressure-driven membrane processes. *Desalination*, 172(1), 85–97.  
<https://doi.org/10.1016/j.desal.2004.07.031>
- [36] Worou, C. N., Chen, Z.-L., & Bacharou, T. (2021). Arsenic removal from water by nanofiltration membrane: Potentials and limitations. *Water Practice and Technology*, 16(2), 291–319.  
<https://doi.org/10.2166/wpt.2021.018>



- [37] Wang, L., Fields, K. A., & Chen, A. S. (2000). Arsenic removal from drinking water by ion exchange and activated alumina plants (p. 147). National Risk Management Research Laboratory, Office of Research and Development, US Environmental Protection Agency.
- [38] Xiao, M., Guo, J., Zhao, S., & Li, S. (2023). Adsorption of As (V) at humic acid-kaolinite-bacteria interfaces: Kinetics, thermodynamics, and mechanisms. *Agronomy*, 13(2), 611. <https://doi.org/10.3390/agronomy13020611>
- [39] Dung, M. D., Nga, T. T. V., Lan, N. T., & Thanh, N. K. (2022). Adsorption behavior and mechanism of As (V) on magnetic Fe<sub>3</sub>O<sub>4</sub>-graphene oxide (GO) nanohybrid composite material. *Analytical Sciences*, 38(2), 427-436. <https://doi.org/10.1007/s44211-022-00064-z>

#### How to cite this paper:



Isloor, A. M., D, M. S., Nayak, S. S., Venkatesh, M. & Shetti, V. (2025). Polydopamine functionalized halloysite nanotubes incorporated polyethersulfone hollow fiber membranes for the removal of arsenic (as-v) from water. *Advances in Environmental Technology*, 11(3), 266-282. DOI: 10.22104/aet.2025.7186.1978